Aerosol and Air Quality Research, 10: 30–37, 2010

ISSN: 1680-8584 print / 2071-1409 online
doi: 10.4209/aaqr.2009.06.0040

Development of a Personal Sampler for Evaluating Exposure to Ultrafine Particles

Masami Furuuchi[1*], Thitiworn Choosong[1], Mitsuhiko Hata[1], Yoshio Otani[1], Perapong Tekasakul[2], Masami Takizawa[1], Mizuki Nagura[1]

[1] *Graduated School of Natural Science and Technology, Kanazawa University, Kakuma-machi, Kanazawa, Ishikawa 9201192, Japan*
[2] *Department of Mechanical Engineering, Faculty of Engineering, Prince of Songkla University, Hat Yai, Songkhla 90112, Thailand*

ABSTRACT

Evaluation of the exposure of humans to ultrafine, airborne particles is an important aspect of health in the workplace, especially in cases where nano-particles are present. However, portable sampling devices for efficiently collecting ultrafine particles in a worker's breathing zone are not readily available. The present study describes the design and development of a portable sampler for collecting particulates in the breathing zone, as a possible tool for this purpose. The design is based on the use of an "Inertial Filter" to separate various-sized nano-order particles. Inertial filters consisting of SUS fiber felt (fiber diameter 5.6–13.5 μm) placed in circular nozzles (3–6 mm diameter with 4.5 mm length) were used. To achieve the smallest d_{p50} under the allowable pressure drop of a portable pump, the influence of fiber loading on separation performance and pressure drop were investigated. The influence of particle loading was also examined in relation to pressure drop and separation performance. The smallest d_{p50} under the allowable pressure drop (5.7 kPa at 6 L/min) for the battery pump employed was ~140 and 200 nm respectively for SUS fibers of 5.6 and 9.8 μm diameter (particle volume fraction ~0.013). The change in separation performance due to particle loading was confirmed to be acceptable for use under the present conditions. Under these conditions, a sufficient amount of particles can be collected for chemical analyses, e.g., particle-bound PAHs after 6–8 hours of sampling. Hence, the developed sampler has the potential for use in evaluating exposure to ultrafine particles in the breathing zone in the workplace.

***Keywords*:** Personal exposure; Ultrafine particles; Inertial filter; Mass concentration.

INTRODUCTION

To accurately assess the health effects of airborne particulates, it is necessary to first determine the chemical composition of particles with respect to particle size. This is because different-sized particles, when inhaled, are deposited in different regions of the lung. This is particularly important for particles in the ultrafine to nano-size range (< 100 nm). A large proportion of such particles can penetrate deeply within the lungs, eventually reaching the alveolar region. Some of the chemicals in particles that are deposited in the alveoli are readily transferred to the blood and then quickly dispersed throughout the body (Hinds, 1999; Bolch *et al.*, 2001). Unfortunately, fine particles with diameters below 2–3 μm, or $PM_{2.5}$ frequently contain high levels of hazardous chemicals. This is particularly true in the case of particles with diameters less than 1 μm (Spruny, 1999; Maynard and Pui, 2007). In a workplace environment contaminated by wood smoke, for example, more than 18% of the polycyclic aromatic hydrocarbons was concentrated in smoke particles smaller than 0.43 μm (Choosong *et al.*, 2009). An evaluation of the chemical characteristics of ultrafine particles is, therefore, important to understanding the health impact of airborne particulates that enter the respiratory system.

In order to conduct various quantitative analyses of atmospheric fine particles, a relatively large amount of particles, on the order of mg, must be collected by filtering atmospheric air. Although particles smaller than 0.1 μm account for a large proportion of the total population, their mass is very small.Therefore, collecting a sufficient mass of atmospheric nano-particles requires a long sampling time. A number of monitors are available for this purpose, including differential mobility analyzers (DMA) (Knutdon and Whitby, 1975) and low pressure impactors (LPI) (Hering *et al.*, 1978; 1979; Kauppinen and Hillamo, 1989), as well as a nano-multi orifice uniform deposit impactor (nano-MOUDI) (Fang *et al.*, 1991; MSP, 2009). However,

* Corresponding author. Tel./Fax: +81-76-2344646
E-mail address: mfuru@t.kanazawa-u.ac.jp

these devices all have drawbacks, such as a small sampling rate, low charging efficiency for nano-particles, the production of artifacts and the loss of unstable chemicals by evaporation due to a large pressure drop (Hata *et al.*, 2009).

The inertial filter was developed by Otani *et al.* (2007) as a technology to overcome these difficulties. The filter has some significant advantages over other techniques, such as a nano-size cutoff diameter under a moderate pressure drop (< 20–30 kPa), as well as a sufficient flow rate that permits the rapid collection of particles. The inertial filter consists of thin, stiff fibers with diameters in the micrometer order, loosely packed in a nozzle that functions under a rather large filtration velocity of ca. 10–50 m/s (Otani *et al.*, 2007). By selecting the appropriate filter structure and filtration conditions, such as filtration velocity, fiber diameter and fiber volume fraction, particles can be classified using inertial filters with cutoff sizes ranging from ca. 50–200 nm. By combining the inertial filter with impactor stages for particles larger than 0.5–1 μm, a sampler applicable to field use was developed and tested under various atmospheric environments (Furuuchi *et al.*, 2007, 2008; Hata *et al.*, 2009). However, workers are generally exposed to varying pollutant concentrations from almost background level to very high levels, resulting in exposures that deviate significantly from the workplace average (e.g., Choosong *et al.*, 2009). Hence, an accurate evaluation of exposure to pollutants in the breathing zone is essential when the health impact of ultrafine airborne particles is an issue. For this purpose, a portable personal sampler with a battery pump that is capable of collecting ultrafine particles down to the nano-size range is needed. However, no such equipment is currently available. The inertial filter technology has the potential for use as a personal sampler, but difficulties exist, due to the requirements that the sampler be portable.

In this study, a new type of personal sampler was developed, based on inertial filter technology, to evaluate exposure to ultra-fine particles (down to the nano-size range) in the breathing zone. Inertial filters consisting of SUS fiber felt of different fiber diameters (fiber diameter 5.6–13.5 μm) placed in circular nozzles were prepared and the influence of fiber loading on separation performance and pressure drop was examined in an attempt to achieve the smallest d_{p50} under the allowable pressure drop of a portable pump. The influence of particle loading was also examined in relation to pressure drop and separation performance.

DESIGN OF THE PERSONAL SAMPLER

Sampler Requirements

The requirement that the personal samplers be portable introduces limitations due to the maximum pressure drop and flow rate of portable battery-operated pumps. The required maximum flow rate is usually less than 10–15 L/min for unloaded conditions under a small allowance of pressure drop less than, e.g., 6–7 kPa. In addition, the quantity of particles collected during a typical working period (~8 hrs) should be sufficient for the subsequent analysis of particle-bound chemicals. The performance of the sampler should not vary significantly during the sampling period due to an increase in particle loading. In addition, personal sampling equipment should preferably be lightweight and compact in size. These practical requirements all represent impediments to designing a functional sampling device.

Although the inertial filter provides a nano-order cutoff size with a lower pressure drop (< 20–30 kPa) than current methods applicable to the nano-size range, such as LPI (70–80 kPa) and nano-MOUDI (~60 kPa) (Fang *et al.*, 1991; Otani *et al.*, 2007), minimization of the pressure drop is essential because of the requirements described above. Moreover, an increase in pressure drop due to particle loading has been shown to be inevitable for the inertial filter (Nagura *et al.*, 2009). Hence, to reduce the pressure drop as much as possible and to also minimize the influence of the re-suspension or bouncing of particles, an inertial filter was with a cutoff size of 0.5–0.7 μm and pressure drop of less than ~0.3 kPa was used as a pre-filter, taking into account the pump capacity. The pre-filter was placed upstream of an inertial filter designed for the ultra-fine range, designated as "the main filter." The use of the inertial filter as a pre-filter may also provide the benefit of compact geometry and less pressure drop than an impactor.

Design of the Inertial Filter

Typical collection efficiency curves for an inertial filter are shown in Fig. 1 (Otani *et al.*, 2007). Large particles are collected by a conventional filter by inertial impaction at a high filtration velocity, while small particles are removed by Brownian diffusion, as shown in Fig. 1. The parameters involved in inertial impaction and Brownian diffusion are the Stokes number, *Stk*, and the Peclet number, *Pe*:

$$Stk = \frac{C_c \rho_p d_p{}^2 u}{9 \mu d_f} \tag{1}$$

$$Pe = \frac{u d_f}{D} \tag{2}$$

where C_c is the Cunningham slip correction factor, ρ the particle density, d_p the particle diameter, u the filtration velocity, μ the viscosity, d_f the fiber diameter, and D the Brownian diffusivity of particles. The collection efficiency of a filter increases with increasing *Stk* and decreasing *Pe*. Therefore, an extremely high filtration velocity and a thin fiber are capable of providing a large inertial effect. This can change a typical collection efficiency curve with the most penetrating particle size. As denoted by the dotted curve in Fig. 1, the collection efficiency for larger particles increases while that for smaller particles decreases. Hence, the collection efficiency curve approaches an ideal classification of particles with d_{p50} in the nano to ultrafine

range. In this study, inertial filters were designed using equations based on filtration theory for a single fiber, as described in previous reports (Otani *et al.*, 2007; Eryu *et al.*, 2009).

Fibers for the Inertial Filter and Equipped Devices

Inertial filters consisting of webbed stainless steel fibers (Nippon Seisen Co. Ltd., felt type, SUS-304) were fixed into a circular nozzle using a resin (polyoxymethylene, POM) separable cassette (see Fig. 2). Since the web of SUS fibers has a high mechanical strength against compression, the filter structure can be maintained at high filtration velocities, and the filtration velocity through the filter at a given pressure drop through the filter remains high. Three different diameters of SUS fiber were used, where the fiber diameter was measured through SEM photographs and shown to have a near lognormal distribution. The filter retainer on the cassette bottom was designed to hold the fiber web by 0.2 mm diameter crossed wires, in order to achieve as small a pressure drop as possible. An inertial filter cassette was employed to make handling of the sampler easier. In addition, they can be easily exchanged with new ones on site without directly touching the fibers. They can be reused after cleaning and are disposable. The specifications of the inertial filters used are summarized in Table 1.

A schematic diagram of the devised sampler, which consists of an inlet nozzle, inertial filters aligned in series, and a filter holder, is shown in Fig. 3. Duralumin and resin (POM) parts were used to reduce the weight of the sampler to below ~150 g. It can be clipped to a chest pocket using an inlet holder. A portable battery pump (SKC, Leland Legacy, 5–15 L/min, 1.0 kg of weight) was employed and connected to the sampler via a PVC tube. This pump was selected because it is ranked as one of the commercially available battery pumps with the largest capacity and is capable of operating 24 hrs on its internal battery.

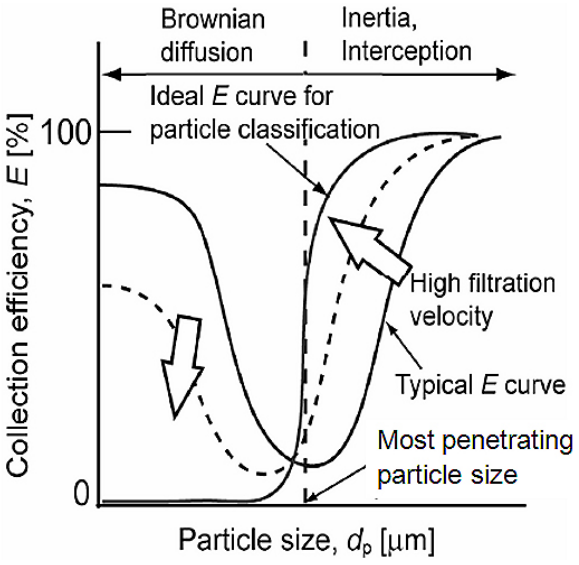

Fig. 1. Aerosol collection efficiency based on inertial filtration (Otani *et al.*, 2007).

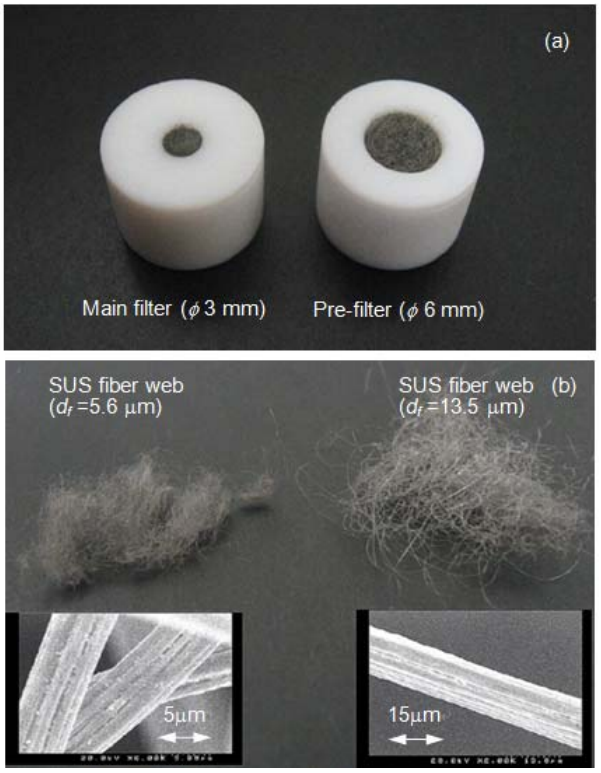

Fig. 2. Inertial filter cartridges for pre and main filters along with SUS fiber web: (a) SUS fiber webs loaded in cassettes, (b) detail of SUS fibers.

EXPERIMENTS

Separation Performance of Inertial Filters and Characteristics of the Test Particles

Fig. 4 shows a schematic diagram for the performance test rig for the inertial filters. Zinc chloride test ($ZnCl_2$) particles (< 300 nm in Stokes' diameter) generated by an evaporation- condensation type aerosol generator and ambient particles (> 300 nm in the optical diameter) were used. Zinc chloride dosed on an alumina boat was heated to 260–320°C in an infrared ray image furnace (ULVAC, RHL-E25P) to the point of evaporation, then cooled to room temperature for condensation, similar to previous reports (Kousaka *et al.*, 1982; Okuyama *et al.*, 1986; Alonso *et al.*, 2004; Otani *et al.*, 2007). Since the generated $ZnCl_2$ particles may form aggregates, their actual density was measured using the "Aerosol Particle Mass Analyzer" (APM), (Kanomax, APM3600), which is capable of measuring a particle mass down to 25 nm (Park *et al.*, 2004a, 2004b; Fukushima *et al.*, 2007; Lee *et al.*, 2009). The average density of 50–100 nm of singly charged $ZnCl_2$ particles generated at 320–350°C was 1865±42 kg/m^3, while the density of pure $ZnCl_2$ is 2907 kg/m^3 (Perry, 1950).

Poly-dispersed $ZnCl_2$ particles were charged by exposure to ^{241}Am, then sized using a differential electrical mobility analyzer (DMA) (TSI, Model 3081) used in a scanning mobility particle sizer (SMPS) (TSI, Model 3936). The mono-dispersed aerosol from the DMA was diluted with l

Table 1. Specification of inertial filter and experimental conditions.

Inlet	Inertial filter	d_f (μm)	Fiber material	Type	L_n (mm)	D_n (mm)	Q (L/min)	Fiber Loadings (mg)	Fiber volume faction α (-)	Cutoff size (field test) (nm)
No. 1	Pre	13.5 (σ_g = 1.1)	SUS-304	web	5.5	6	6	14.7–18.2	0.0143	700
	Main	9.8 (σ_g = 1.1)			4.5	3	6	3.2–3.5	0.0135	200
No. 2	Pre	9.8 (σ_g = 1.1)	SUS-304	web	5.5	6	6	20.4–22.7	0.0165	700
	Main	5.6 (σ_g = 1.1)			4.5	3	6	1.6–4.2	0.0128	140

d_f: fiber diameter; D_n: nozzle diameter; L_n: nozzle length; Q: flow rate
α: values used for filed test, Fiber density: 7980 kg/m^3 Young's modulus of SUS304: 199.14 Gpa

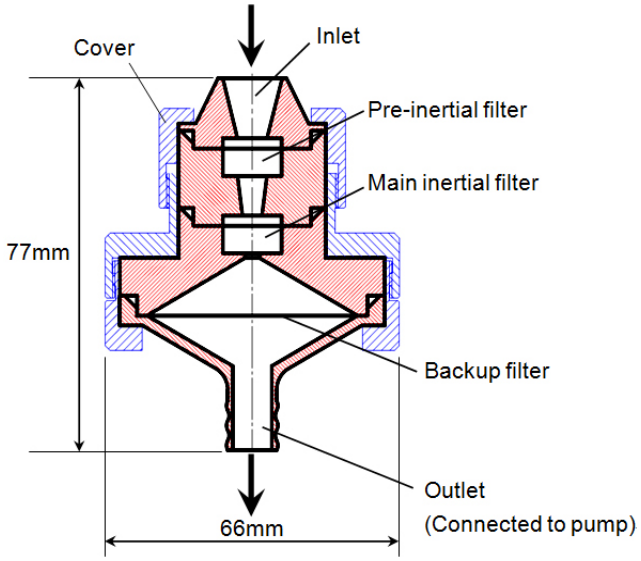

Fig. 3. Schematic diagram of the developed personal aerosol sampler.

air filtered through a HEPA filter and then supplied to the inertial filter, which was installed in a holder with a nozzle inlet, at a flow rate of 6 L/min. The collection efficiency on a particle number basis was determined using an aerosol electrometer (TSI, Model 3068), based on the measured current ratio upstream and downstream from the inertia filter. Pressure drop through the inertial filter was measured by means of a digital manometer (Sokken, Model PE-33-A1).

The pressure drop through the inertial filter is closely related to separation behavior. Hence, the filtration velocity and quantity of fiber used must be selected with care. Fig. 5 shows the measured performance curve of the pump used. Linearity between flow rate and allowable pressure drop was observed. The total pressure drop through the sampler must be lower than this curve for a given flow rate. Under this limitation, a separation performance test was performed by changing the fiber loading and flow rate to determine the smallest d_{p50} with an acceptable pressure drop through the main inertial filter. In the present study,

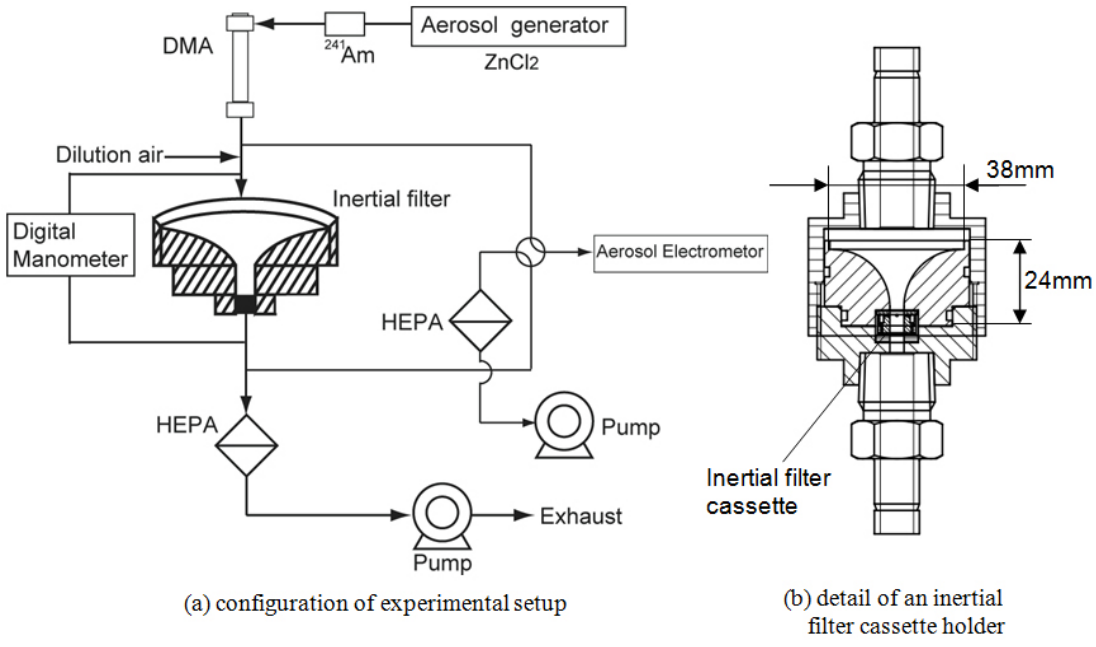

Fig. 4. Experimental setup for the filter performance test: (a) configuration of setup, (b) detail of an inertial filter cassette holder.

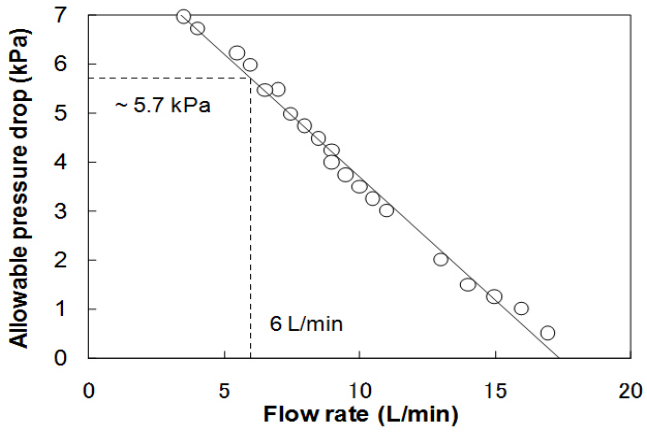

Fig. 5. Allowable pressure drop a portable pump used in relation to flow rate.

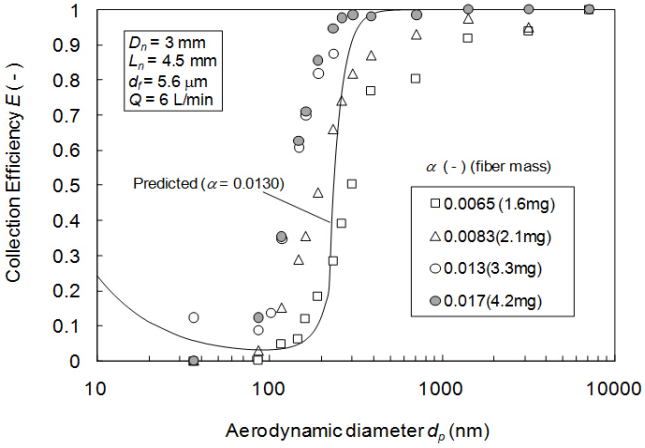

Fig. 6. Collection efficiency of the main inertial filter at various fiber loadings.

this condition was determined to be 6 L/min with 5.7 kPa. An increase in pressure drop due to particle loading was also taken into account in this condition. The experimental conditions are also shown in Table 1.

An increase in pressure drop due to particle loading was also examined through a lab scale particle loading test using incense smoke particles. A box chamber (70 × 70 × 100 cm), in which some pieces of thin rod incense were burned, was used as an aerosol source. Sampler (No. 1) was connected to the chamber top via a tube. Clean air was introduced through an inlet with a HEPA filter on the box side during the sampling. The sampling period was set as 7 min. The particle concentration was adjusted to produce different particle loadings by changing the amount of incense used. After collecting the smoke particles, the total pressure drop through the sampler was measured using the digital manometer described above. Binder-less quartz fiber filters (Pallflex 2500QAT-UP) were used for the backup filter taking into account the application to field measurements. All filters, including the inertial filter cassettes, were conditioned in a desiccator at ~23°C and ~50% relative humidity for at least 48 hours. They were then weighed to obtain the initial weights. After measuring the pressure drop, they were weighed again after 48 hours under the same conditioning procedures.

RESULTS AND DISCUSSION

Separation Performance of the Inertial Filters

Fig. 6 shows separation efficiency curves for the main inertial filter (No. 2) measured for different fiber loadings at a flow rate of 6 L/min using the experimental setup shown in Fig. 4. The collection efficiency is plotted on the basis of the aerodynamic diameter (< 300 nm) and optical diameter (> 300 nm). Solid curves were calculated from theoretical predictions in which the main collection mechanisms, inertia, diffusion and interception were taken into account, for a single fiber (Otani *et al.*, 2007; Eryu *et al.*, 2009). The cutoff size, or d_{p50}, decreased to ~130 nm with increasing fiber loading. This size corresponds to a Stoke's diameter of ~80 nm (Hinds, 1999) for a singly charged particle. The separation curves subsequently became steeper. For particle sizes below 30–40 nm, the collection efficiency increased slightly because of the increasing influence of diffusion (Otani *et al.*, 2007). Separation performance is described theoretically for this condition, although the cutoff size is overestimated by 70–80%. The reason for this was not investigated in this study. However, it might be related to an effect similar to that for the aerosol dynamic lens (Wang and McMurry, 2006). That is, an aerosol with a large filtration velocity may be focused after passing through each fiber. This may cause an increase in single fiber collection efficiency.

Because the effect of diffusion increases with a smaller Peclet number, as well as the interception effect, the collection efficiency for nano-particles less than ~30 nm increases (Otani *et al.*, 2007; Eryu *et al.*, 2009). This results in a decrease in the degree of penetration of nano-particles. When the number of particles in this range is important, such an increase should not be evident. However, most of the particle mass below this cutoff can be collected as the remaining negligible mass of particles below 20–30 nm under this condition.

Separation curves for different sets of inertial filters (No. 1 and 2) listed in Table 1 are shown in Figs. 7(a) and (b). The solid curves describe tendencies. Both filter-sets provided similar separation behaviors. However, the use of a finer fiber (d_f = 5.6 μm) in the main inertial filter resulted in a smaller d_{p50} (~140 nm) with a steeper separation curve. The pre-filters have almost the same d_{p50} (~700 nm) and the separation curves are similar. The collection efficiency of particles larger than ~1 μm appears to decrease, as the result of bouncing. Hence, the inertial filter should be used judiciously for this range of particles because of the increased risk of re-suspension or bouncing. The experimentally estimated d_{p50} for each inertial filter are summarized in Table 1.

Pressure Drop and Influence of Particle Loading

In Fig. 8, both the d_{p50} for the main inertial filter (No. 1) and the total pressure drop are plotted against the amount

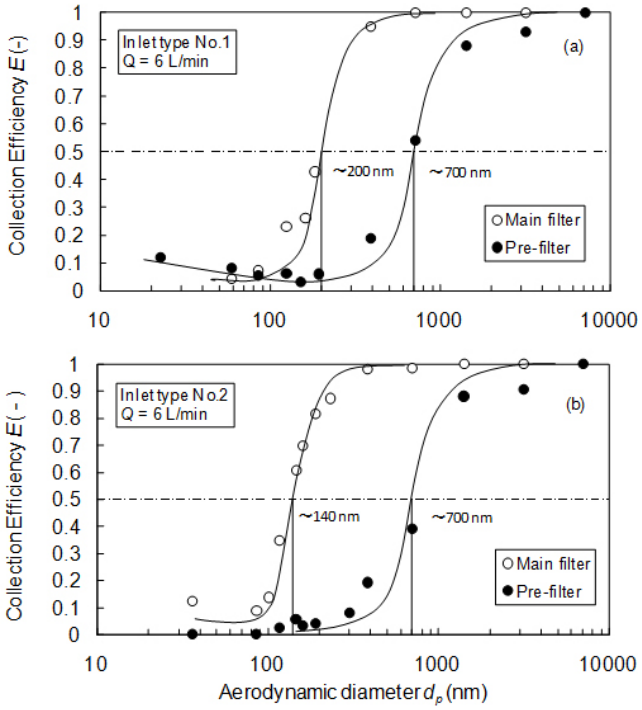

Fig. 7. Collection efficiency curves of inertial filters used in field tests: (a) tunnel (inlet type No.1) and (b) train cabin (inlet type No.2).

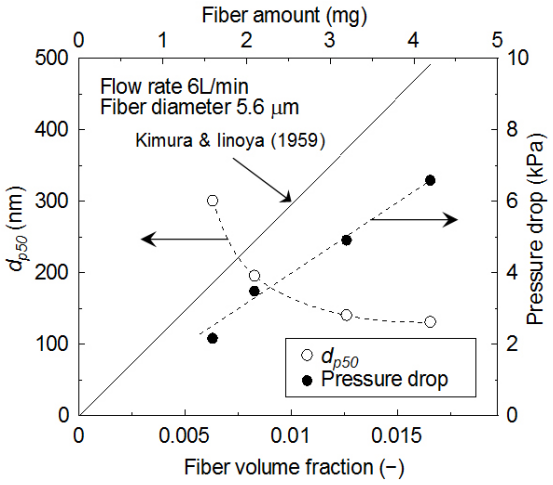

Fig. 8. Cutoff size and pressure drop through inertial filter in relation to loaded fiber amount (fiber diameter d_f = 5.6 μm).

of fiber web loaded. These data were measured at a fiber diameter of 5.6 μm and an air flow rate of 6 L/min. The solid line denotes the prediction based on Kimura and Iinoya's equation (Kimura and Iinoya, 1959). The d_{p50} decreased with increased fiber loading, or the fiber volume fraction. However, it leveled off at over 4 mg of fiber loading. The pressure drop increased with fiber loading and exceeded 5 kPa for a loading of 4 mg or greater. The measured pressure drops were slightly lower the values predicted by Kimura and Iinoya's equation. This might be related to the actual packing structure of the fiber web, i.e., to fiber orientation, contact between fibers and non-uniformity. The collection efficiency curve for the main inertial filter (No. 2) (d_f = 5.6 μm, fiber volume fraction = 0.013), shown in Fig. 7(b), corresponded to a pressure drop of less than 5 kPa, taking into account an increase in the pressure drop due to particle loading. This is within the maximum allowable pressure drop (5.7 kPa at 6 L/min).

Fig. 9 shows the relationship between the total pressure drop through the sampler including inertial filters (No. 1: d_{p50} ~200 nm), a quartz fiber filter on the filter holder with tubing, and the particle mass loading on each filter. Data from particle loading tests using incense smoke were used. The total pressure drop increased with total particle loading. However, the particle loading in the pre-filter (0.06–1.2 mg) did not contribute significantly to the total pressure drop. As a result, the correlation is not clear. The influence of particle loading was dominant at the main inertial filter and backup filter (BK), but still less than 5 kPa, even for a ~7 mg particle loading. For the inertial filter with d_{p50} = ~140 nm, the increase in pressure drop was estimated to be ~0.2 kPa after 0.5 mg of particle loading assuming a similar increase with particle loading to d_{p50} = ~200 nm. This indicates that the present designing conditions of 6 L/min with d_{p50} = 140 and 200 nm can provide a sufficient margin for the allowable pressure drop.

Particle loading may also influence separation performance, such as d_{p50}. The influence of particle loading on the performance of inertial filters has been investigated previously (Nagura *et al.*, 2007). According to this investigation, the separation performance of an inertial filter did not change greatly when fine particles such as cigarette smoke particles were filtered through inertial filters (both 5.6 and 9.8 μm) at a filtration velocity of 10–37.5 m/s. They concluded that particles are deposited only around the stagnation point of the fibers, which does not have a significant effect on collection efficiency. The filtrating conditions for the developed samplers (filtration velocity = 14.1 m/s, fiber volume fraction ~0.01, fiber diameter 5.6 and 9.8 μm) were in the above range. Hence, the influence of particle loading on separation performance may not be of great significance in the present case. The penetration of ultrafine particles through the main inertial filter (< ~200 nm) using sampler No.1 remained essentially unchanged (0.62 ± 0.09) for particle loadings below ~0.3 mg. A further increase in particle loading may cause a decrease in penetration due to a decrease in the d_{p50}. Under this condition, however, particle loading on the backup filter is sometimes in a range sufficient for the analysis of chemicals, e.g., polycyclic aromatic hydrocarbons (PAHs) in ambient particles.

CONCLUSION

This study describes the design of a device that permits the exposure of humans to airborne ultrafine particles to be evaluated. A method for capturing particles that can be

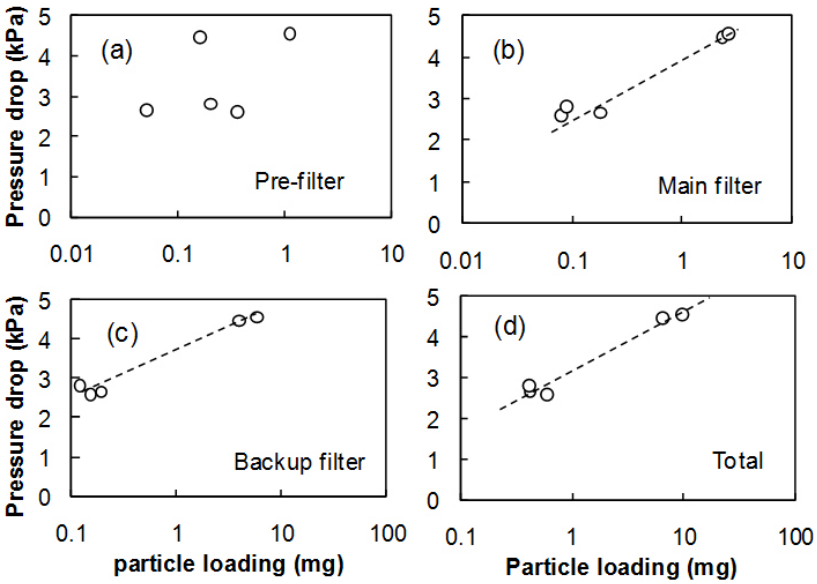

Fig. 9. Increase in pressure drop with particle loading for the aerosol sampler (type No.1).

inhaled by humans under working conditions is critical to evaluating the health-related impact of such particles. To accomplish this, a portable sampler for evaluating the exposure of workers to ultra-fine particles, based on "Inertial Filter" technology, was developed. The smallest d_{p50} under the allowable pressure drop (5.7 kPa at 6 L/min) of the battery pump employed was ~140 and 200 nm respectively for SUS fibers with diameters of 5.6 and 9.8 μm (particle volume fraction ~0.013). Changes in separation performance due to particle loading was confirmed to be sufficiently small under the conditions used. Under these conditions, the amount of particles that can be collected is sufficient for chemical analysis, e.g., particle-bound PAHs after 6–8 hours of sampling. The developed sampler satisfies the requirements for a personal sampler in that is compact and lightweight (~1 kg), including a battery pump. The filter cassette geometry employed provides flexibility and ease of use. As a result, the sampler has the potential for use in evaluating exposure to ultrafine particles in the breathing zone.

Using the developed sampler, field tests were conducted under various conditions to demonstrate the importance of evaluating the exposure of workers to ultrafine particles. These results will be reported in the near future. One of the important remaining issues related to the sampler is to further improve the d_{p50} down to 100 nm or smaller. This is important in terms of obtaining detailed information on the characteristics of nano-size particles. This may be done primarily by decreasing the pressure drop through the inertial filter, since the capacity of portable pumps has been exploited to the maximum. This improvement based on the use of an inertial filter with a different structure is currently in progress.

ACKNOWLEDGEMENTS

The authors would gratefully acknowledge The Japan Society for the Promotion of Science (JSPS) for its support for this research (grant No. 20651007).

REFERENCES

Alonso, M., Alguacil, F.J. (2006). Thin Coating on Ultrafine Aerosol Particles. 16th International Conference on Nucleation and Atmospheric Aerosols - ICSB 2004. *Atmospheric Research*. 82: 605-609.

Bolch, W.E., Farfan, E.B, Huh, C., Huston, T.E., Bolch, W.E. (2001). Influence of Parameter Uncertainties within the ICRP 66 Respiratory Tract Model: Particle Deposition. *Health Phys.* 81: 378-394.

Choosong, T., Chomanee, J., Tekasakul, P., Tekasakul, S., Otani, Y., Hata, M. and Furuuchi, M. (2009). Workplace Environment and Personal Exposure of PM and PAHs to Workers in Natural Rubber Sheet Factories Contaminated by Wood Burning Smoke. *Aerosol Air Qual. Res.* 10: 8-21

Choosong, T., Nagura, M., Takizawa, M., Hata, M., Otani, Y., Bai, Y. and Furuuchi, M. (2008). Development of a New Personal Sampler for Evaluation of Exposure for Aerosol Nano-particles, Proc. International Aerosol Symposium 2008, Kanazawa. p. 267-268. (in Japanese).

Eryu, K., Seto, T., Mizukami, Y., Nagura, M., Furuuchi, M., Tajima, Y., Kato, T., Ehara, K. and Otani, Y. (2009). Design of Inertial Filter for Classification of $PM_{0.1}$. *J. Aerosol Res.* 24: 24-29. (in Japanese).

Fang, C.I., McMurry, P.H., Marple, V.A. and Rubow, K.L. (1991). Effect of Flow-induced Relative Humidity Changes on Size Cuts for Sulfuric Acid Droplets in the MOUDI. *Aerosol Sci. Technol.* 14: 266-277.

Fukushima, N., Ehara, K., Sakurai, H. and Coakley, K.J. (Ed.) Development of the Aerosol Particle Mass Analyzer, Proc. 25th Annual Tech. Meeting on Air Cleaning and Contamination Control, Tokyo, 2007, p. 128-130. (in Japanese).

Furuuchi, M., Choosong, T., Tekasakul, P., Yoshikawa, F., Tekasakul, S., Hata, M. and Otani, Y. (Ed.). Worker's Exposure to Nano Smoke Particles from Wood Burning in A Rubber Sheet Smoking Factory. Proc. The 3rd International Symposium on Nanotechnology, Occupational and Environmental Health, Taipei, Taiwan, 2007, p. 304-305.

Furuuchi, M., Otani, Y., Nakao, Y., Tsukawaki, S., Hang, P. and Sieng, S. (Ed.). Characteristics of PAHs in Ambient Aerosol Particles Collected by $PM_{0.1}$ Sampler with Inertial Filter. Proc. Asian Aerosol Conference (AAC) 2007, Kaoshung, Taiwan, 2007, p. 41-42.

Hata, M. Bai, Y., Yoshikawa, F., Fukumoto, M., Otani, Y., Sekiguchi, K., Tajima, Y. and Furuuchi, M. (2009). Characteristics of Aerosol Nano-Particles Sampled at Road Tunnel and Roadside in Kanazawa Outer Ring. *Bulletin of the Japan Sea Res. Inst.* 40: 31-36. (in Japanese)

Hata, M., Bai, Y., Furuuchi, M., Fukumoto, M., Otani, Y., Sekiguchi, K. and Tajima, N. (2009). Status and Characteristics of Ambient Aerosol Nano-particles in Kakuma, Kanazawa and Comparison between Sampling Characteristics of Air Samplers for Aerosol Particle Separation. *Bulletin of the Japan Sea Res. Inst*. 40: 135-140. (in Japanese)

Hering, S.V., Flagan, R.C. and Fliedlander, S.K. (1978). Design and Evaluation of New Low-Pressure Impactor. *Environ. Sci. Technol.* 12: 667-673.

Hering, S.V., Fliedlander, S.K., Collins, J.J. and Richards, L.W. (1978). Design and Evaluation of a New Low-Pressure Impactor 2. *Environ. Sci. Technol.* 13: 184-188.

Hinds, W.C. (1999). *Aerosol Technology*, 2nd ed., Wiley-Interscience, New York.

Kauppinen, E.I. and Hillamo, R.E. (1989). Modification of the University of Washington Mark 5 in-stack Impactor. *J. Aerosol Sci.* 20: 813-827.

Kimura, N. and Iinoya, K. (1959). Experimental Studies on the Pressure Drop Characteristics of Fiber Mats. *Kagaku Kogaku*. 23: 792-798. (in Japanese)

Knutdon, E.O. and Whitby, K.T. (1975). Aerosol Classification by Electric Mobility: Apparatus, Theory, and Application. *J. Aerosol Sci.* 6: 443-451.

Kousaka, Y., Niida, T., Okuyama, K. and Tanaka, H. (1982). Development of a Mixing Type Condensation Nucleus Counter. *J. Aerosol Sci.* 13: 231-240.

Larsen, J.C. and Larsen, P.B. (1998). In *Air Pollution and Health—Chemical Carcinogens.* Hester, R.E., Harrison, R.M. (Eds.), Cambridge, UK: Royal Society of Chemistry. p. 33-56.

Lee, S.Y., Widiyastuti, W., Tajima, N., Iskandar, F. and Okuyama, K. (2009). Measurement of the Effective Density of Both Spherical Aggregated and Ordered Porous Aerosol Particles Using Mobility- and Mass-Analyzers. *Aerosol Sci. Tech.* 43: 36 -144.

Mayland, A.D. and Pui, D.Y.H. (2007). *Nanoparticles and Occupational Health*. Splinger. Dordrecht.

MSP. (2009). http://www.mspcorp.com/aero_products.php.

Nagura, M., Mizukami, Y., Eryu, K., Otani, Y. and Seto, A. (Ed.). Influence of Particle Loadings on the Separation Characteristics of Inertial Filter. Proc. 73th Annual Meeting of Society of Chemical Engineers in Japan, Hamamatsu, B104, 2009. (in Japanese)

Nisbet, C. and LaGoy, P. (1992). Toxic Equivalency Factors (TEFs) for Polycyclic Aromatic Hydrocarbons (PAI-Is). *Regul. Toxicol. Pharm.* 16: 290-300.

Okuyama, K., Kousaka, Y. and Hayashi, K. (1986). Brownian Coagulation of Two-component Ultrafine Aerosols. *J. Colloid Interface Sci.* 113: 42-54

Otani, Y., Eryu, K., Furuuchi, M., Tajima, N. and Tekasakul, P. (2007). Inertial Classification of Nanoparticles with Fibrous Filters. *Aerosol Air Qual. Res.* 7: 343-352.

Park, K., Kittelson, D.B. and McMurry, P.H. (2004a). Structural Properties of Diesel Exhaust Particles Measured by Transmission Electron Microscopy (TEM): Relationships to Particle Mass and Mobility. *Aerosol Sci. Technol.* 38: 881-889.

Park, K., Kittelson, D.B., Zachariah, M.R. and McMurry, P.H. (2004b). Measurement of Inherent Material Density of Nanoparticle Agglomerates. *J. Nanopart. Res.* 6:267-272.

Perry, J.H. (1950). *Chemical Engineer's Handbook*, 3rd ed. McGraw-Hill. New York. p. 148.

SKC. (2009). http://www.skcinc.com/index.asp.

Spurny, K.R. (1999). *Analytical Chemistry of Aerosols*. Lewis. Boca Raton.

Wang, X. and McMurry, P.H. (2006). A Design Tool for Aerodynamic Lens Systems. *Aerosol Sci. Tech.* 40: 320-334.

Received for review, June 2, 2009
Accepted, July 31, 2009